JOURNAL OF NANO- AND ELECTRONIC PHYSICS
Vol. **5** No 4, 04061(6pp) (2013)

ЖУРНАЛ НАНО- ТА ЕЛЕКТРОННОЇ ФІЗИКИ
Том **5** № 4, 04061(6cc) (2013)

Elastic, Optoelectronic and Thermal Properties of Boron Phosphide

S. Daoud[1,*], N. Bioud[2,†] L. Belagraa[3], N. Lebgaa[2]

[1] *Faculté des Sciences et de la Technologie, Université de Bordj Bou Arreridj, 34000, Algérie*
[2] *Laboratoire d'Optoélectronique et Composants, Université Ferhat Abbes- Sétif, 19000, Algérie*
[3] *Laboratoire Matériaux et Systèmes Electroniques, Université de Bordj Bou Arreridj, 34000, Algérie*

(Received 02 March 2013; revised manuscript received 18 April 2013; published online 31 January 2014)

Elastic, mechanical, optoelectronic and some thermal properties of boron phosphide (BP) in its structure zincblende phase has been performed using the pseudopotential combined with the plane wave method. The plane-wave pseudopotential approach to the density-functional theory within the local density approximation (LDA) implemented in Abinit code is used. The elastic stiffness and compliance constants, bulk modulus, shear modulus, zener anisotropy factor, young's modulus, internal strain parameter, poisson's ratio, sound velocity for directions within the important crystallographic planes, Debye temperature, melting point, refractive index, plasmon energy, force constants, lattice energy, band gap energy, homopolar energy, heteropolar energy, ionicity and dielectric constant are obtained and analyzed in comparison with the available data.

Keywords: Elastic, Optoelectronic and thermal properties, (B3) BP.

PACS numbers: 45.10. Ab, 62. 20. Dx, 81.40.Jj

1. INTRODUCTION

Several works [1-11] have studied structural, elastic, and electronic properties of boron phosphide com-pound. The ground state, and the high-pressure effect have been calculated by Wentzcovitch et al. [1], using the plane-wave basis sets and pseudopotential appr-oach (PW-PP) within the local density approxi-mation (LDA). Using the linear muffin-tin orbitals (LMTO) method within the LDA, the structural prope-rties of BP have been determined by Lambrecht et al. [2]. The electronic structure and phase transition under high pressure have been studied by Zaoui et al. [3], using the linearized augmented plane-wave (LAPW) method within the generalized gradient approximation (GGA). H. Meradji et al. [6] have used the full-potential density functional method to study the electronic and structural properties of BP for both zincblende and rock salt structures utilizing a hybrid full-potential linear augmented plane-wave plus local orbitals (LAPW+lo) method.

In this work, we report numerical study of elastic properties, sound velocity, Debye temperature, melting point, refractive index, plasmon energy, force constants, lattice energy, band gap energy, homopolar energy, heteropolar energy, ionicity, and dielectric constant of boron phosphide compound in its structure zincblende phase (B3).

2. SIMULATION PROCEDURE

The calculations were obtained using the pseudopotential method combined with the plane waves approach based on density functional theory [12], implemented in the ABINIT code [13, 14]. ABINIT code is a package whose main program allows one to find the total energy, charge density, electronic structure and several other physical properties of systems (molecules and periodic solids) within density func-tional theory, using pseudopotentials and a plane-wave basis-set. It is a common project of the Université Catholique de Louvain, Corning Incorporated, the Université de Liège, and other contributors.

We used the Teter and Pade parameterization [15] for LDA. Only the outermost electrons of each atom were explicitly considered in the calculation. The effect of the inner electrons and the nucleus (the frozen core) was described within a pseudopotential scheme. We used the Trouiller Martins scheme [16] to generate the norm -conserving nonlocal pseudopotential, which results, in highly transferable and optimally smooth pseudo-potentials. A plane-wave basis set was utilized to solve the Kohn-Sham equations in the pseudopotential implementation of the DFT-LDA.

The parameters that affect the accuracy of calculations are the energy cut-off and the number of special k-points used for the Brillouin zone (BZ) integration. The Brillouin zone integrations were replaced by discrete summations over a special set of k-points, using the standard k-point technique of Monkhorst and Pack [17]. Where the k-point mesh used is $(4 \times 4 \times 4)$. The plane-wave energy cutoff to expand the wave functions is set to be 60 Hartree. The relative energy converged to better than 10^{-5} eV/atom.

3. DISCUSSION OF RESULTS

3.1 Elastic and Mechanical Properties

3.1.1 Elastic Stiffness Constants

The number of elastic stiffness constants is usually reduced if the crystal possesses symmetry elements, and in the case of cubic crystals there are only three independent stiffness constants. The array of values of the elastic stiffness constant is therefore reduced for a cubic crystal to the following matrix [C] [18].

* salah_daoud07@yahoo.fr
† b_nadhira1@yahoo.fr

$$[C]=\begin{bmatrix} C_{11} & C_{12} & C_{12} & 0 & 0 & 0 \\ C_{12} & C_{11} & C_{12} & 0 & 0 & 0 \\ C_{12} & C_{12} & C_{11} & 0 & 0 & 0 \\ 0 & 0 & 0 & C_{44} & 0 & 0 \\ 0 & 0 & 0 & 0 & C_{44} & 0 \\ 0 & 0 & 0 & 0 & 0 & C_{44} \end{bmatrix}, \quad (1)$$

In a cubic lattice, three independent elastic constants C_{11}, C_{12}, and C_{44} are determined by employing suitable lattice distortions. Following the work of Nielsen and Martin [19], we determine these constants (*for more details and informations about this method see for example, our previous work: S. Daoud, K. Loucif, N. Bioud, N. Lebgaa and L. Belagraa, Pramana J. Phys.* ***79****, 95 (2012), or also the following paper: K. Bouamama, N. Lebgaa and K. Kassali, High Pressure Res.* ***25*** *(3), 217 (2005)*). The obtained elastic stiffness constants C_{11}, C_{12}, and C_{44}, of (B3) BP at zero-pressure are listed in table 1, and compared with other experimental [5] and theoretical [6-10] data. For cubic crystals, the bulk modulus B is related to the elastic constants by:

$B = (C_{11} + 2C_{12})/3$. The requirement of mechanical stability in a cubic crystal leads to the following restrictions:

$$C_{11} - C_{12} > 0,\ C_{11} > 0,\ C_{44} > 0,\ \underline{C}_{11} + 2C_{12} > 0.$$

Our constants C_{ij} obey these stability conditions, including that C_{12} is relatively smaller than C_{11}, and meaning that $C_{12} < B < C_{11}$.

3.1.2 Internal Strain Parameter, Shear Modulus and the Isotropy Factor

The internal strain parameter was introduced by Kleinman [20], describing the relative ease of bond bending versus the bond stretching. Minimizing bond bending leads to $\xi = 0$, minimizing bond stretching leads to $\xi = 1$. Later, Harrison [21] linked the Kleinman parameter in an approximated way to the elastic stiffness constants C_{11} and C_{12}: [22]

$$\xi = \frac{(C_{11} + 8C_{12})}{(7C_{11} + 2C_{12})}, \quad (2)$$

The shear modulus Cs and the isotropy factor A in a cubic crystal are respectively defined as [23]

$$C_s = (C_{11} - C_{12})/2, \quad (3)$$

$$A = (C_{11} - C_{12})/2C_{44}, \quad (4)$$

The obtained values of the internal strain parameter ξ, the shear modulus Cs and the isotropy factor A of (B3) BP are also listed and compared with other theoretical and experimental data in Table 1. From the data of the Table 1, it can be seen that our calculated elastic stiff-ness constants C_{11}, C_{12} and C_{44} are in good agreement with the experimental data, they are deviating from the measured values [5] within the range 13.27 %, 16.5 % and 21.62 %, respectively.

3.1.3 Compliance Constants

The elastic compliance tensor [S], which has the same form as [C], is connected reciprocally with the tensor [C] through Hooke's relation. Explicit equations for the component S_{ij} in terms of C_{ij} can be given by the following formulas [23]

$$S_{11} = (C_{11} + C_{12})/[(C_{11} - C_{12})(C_{11} + 2C_{12})], \quad (5\text{-a})$$

$$S_{12} = -C_{12}/[(C_{11} - C_{12})(C_{11} + 2C_{12})], \quad (5\text{-b})$$

$$S_{44} = 1/C_{44}, \quad (5\text{-c})$$

The obtained values of the compliance constants S_{ij} of (B3) BP at zero-pressure are presented in Table 1, and compared with the available theoretical data [11]. According to the data in the Table 1, it can be seen that our calculated compliance constants S_{ij}, are relatively different, in comparison with the values found by the author [11]. It is worth noting also, that the value 1.00 (10^{-2}GPa^{-1}) of S_{44}, obtained in previous work [11], seems to be inaccurate, because the later author used the experimental value (C_{44} = 1.60 Mbar = 160 GPa) of Wettling and Windscheih [5] to estimate the value of S_{44}, and if we use this experimental value (C_{44} = 1.60 Mbar) in the formula (5-c), we obtain the result (S_{44} = 0.625 Mbar^{-1}). Hence, the results found in the present work for the compliance constants S_{11}, S_{12} and S_{44} are deviating from the values of the author [11] by the marked differences of 16.9 %, 35.2 % and 17.8 % respectively.

Table 1 – Some physical parameters of (B3) BP at zero-pressure in comparison with experimental [5] and theoretical [6-11] values.

Parameter	Our work	Other works
C_{11} (GPa)	356.8	315[5] 357[6]LDA 337[6]GGA 359[7] 329[8] 358.9[9] 360[10]
C_{12} (GPa)	83.5	100[5] 87[6]LDA 78[6]GGA 81[7] 97.5[8] 80.6[9] 155[10]
C_{44} (GPa)	194.6	160[5] 150[6]LDA 200[6]GGA 202[7] 154[8] 196.7[9] 146[10]
B (GPa)	174.6	172[2] 173[5] 176[6]LDA 160[6]GGA
C_s (GPa)	136.6	139[7]
ξ	0.384	0.31[7]
A	0.702	0.67[11]
S_{11} (10^{-2} GPa^{-1})	0.3075	0.37[11]
$-S_{12}$ (10^{-2}GPa^{-1})	0.0583	0.09[11]
S_{44} (10^{-2} Gpa^{-1})	0.5138	1.00[11] 0.625[11] (the right value)

3.1.4 Young's Modulus and Poisson's Ratio

Young's modulus Y is not isotropic in cubic zinc-blende type crystals [23]. The Young modulus Y for an arbitrary crystallographic direction m can now be given by [23]

$$\frac{1}{Y} = S_{11} - 2\left(S_{11} - S_{12} - S_{44}\right)\left(m_1^2 m_2^2 + m_2^2 m_3^2 + m_1^2 m_3^2\right), \quad (6)$$

Where the S_{ij} values are the elastic compliance constants and the m, values are the direction cosines for m. Poisson's ratio P also varies with orientation. If a longitudinal stress in the direction m and the transverse strain along the orthogonal direction n are under consideration, then the ratio P can be given by [23]

$$P = -\frac{\left[S_{12} - 2\left(S_{11} - S_{12} - S_{44}\right)\left(m_1^2 m_1^2 + m_2^2 m_2^2 + m_3^2 m_3^2\right)\right]}{\left[S_{11} - 2\left(S_{11} - S_{12} - S_{44}\right)\left(m_1^2 m_2^2 + m_2^2 m_3^2 + m_1^2 m_3^2\right)\right]}, \quad (7)$$

The ratio P, in this case, is written as $P = -S_{12}/S_{11}$ [23]. The variations of Y and P for directions within the important crystallographic planes {100}, {110}, and {111} are given in Table 2, and also compared with the other theoretical data [11]. The data in the Table 2, showed that our values of Y and P for directions are also relatively different compared to the values of the author [11]. This noted difference might be due to the effect of the error in the value ($1\ \text{Mbar}^{-1} = 10^{-2}\text{GPa}^{-1}$) of S_{44}, because all the values of Y and P depend on S_{44}.

Table 2 – Young's modulus Y, and Poisson's ratio P for directions within the important crystallographic planes {100}, {110} and {111} at zero-pressure. [11] Calculated using ($S_{11} = 0.37$, $S_{12} = -0.09$, $S_{44} = 1.0$) (10^{-2}GPa^{-1}) at $T = 300$ K

Plane	Direction	Y (GPa)	
		Our work	Other works
{100}	<001>	325.2	270[11]
	<011>	395.1	260[11]
{110}	<001>	325.2	270[11]
	<111>	425.7	250[11]
{111}		395.1	260[11]
Plane	Direction	Poisson's ratio	
		Our work	Other works
{100}	m = <010>, n = <001>	0.189	0.24[11]
	m = <011>, n = <0 $\bar{1}$ 1>	0.015	0.28[11]
{110}	m = <001>, n = <1 $\bar{1}$ 0>	0.189	0.24[11]
	m = <1 $\bar{1}$ 1>, n = <1 $\bar{1}$ $\bar{2}$ >	0.093	0.26[11]
{111}		0.158	0.25[11]

3.2 Optoelectronic Properties

The result obtained of energy band structure at equilibrium lattice parameter, along the high symmetry directions in the Brillouin zone is shown in Fig. 1(a), the minimum of the conduction band is found to be at the Δ_{min} (near X point), rendering this compound an indirect semiconductor with a big $\Gamma_{15v} \rightarrow \Delta_{min}$ optical transition of 1.20 eV.

The electronic charge density is an important property of solids and can be only described accurately in the context of first-principles studies. The calculated profile valence density charge along the <111> direction is shown in Fig. 1(b), this figure clearly shows that most of the charge is located around the center between the two atoms. The low displacement of valence charge is a natural indication for the small value of ionicity parameter of this compound.

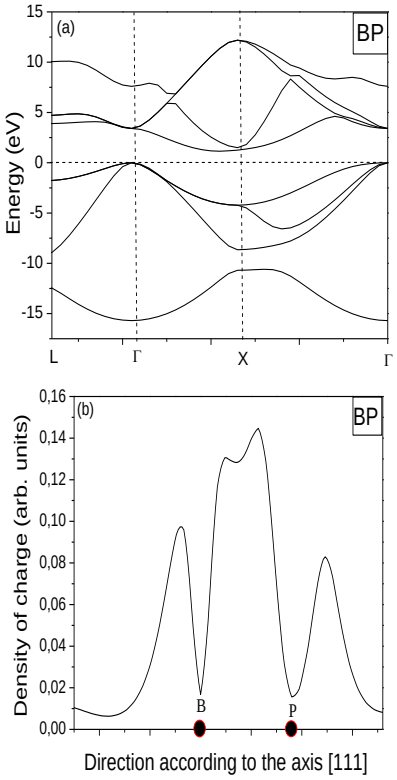

Fig. 1 – Band structure along the principal high-symmetry points of the (B3) BP compound (a), Total valence charge densities along the <111> direction at equilibrium volume (b)

The evaluation of refractive indices of a semiconductor is of considerable importance for many optoelectronic applications, where the refractive index of the mterial is the key parameter for the optoelectronic devices.

Reddy et al. [24] have proposed a relationship between a several physical parameters and the refra-ctive index for the A^{II}-B^{VI} and A^{III}-B^{V} groups of semconductors. Recently, Kumar and Singh [25] gave another relationship between the energy gap and the refractive index for some mixed materials, belonging to groups IV, II-VI and III-V semiconductors, insulators, oxides and halides.

The refractive index of a semiconductor material typically decreases with increasing band gap energy E_g. There are various empirical and semi-empirical rules and expressions that relate n to E_g. The refra-ctive index of (B3) BP, can be estimated by using the following formula [25]

$$n = C_1 E_g^c, \quad (8)$$

where: n is the refractive index, E_g is the average energy gap (in eV), C_1 and c are the constants, they are equal respectively: 3.3668 and – 0.32234.

In Moss' rule, n and Eg are related by: $n^4 E_g = C_2$, C_2 is constant ≈ 100 eV. In the Hervé-Vandamme relationship [26]

$$n^2 = 1 + \left[A_1/\left(E_g + A_2\right)\right]^2, \quad (9)$$

where A_1 and A_2 are constants ($A_1 \approx 13.6$ eV and $A_2 \approx 3.4$ eV).

The values of refractive index n of (B3) BP obtained from the relations of equations (8) and (9) are equal to 3.18 and 3.08 respectively. These two values are in very good agreement with the experimental data. They are deviate from the value 3.34 of the authors [5] within 4.79 % and 7.78 % respectively. The later value (3.34) has been obtained at specified photon energy of 0.37 eV.

The refractive index, versus, the plasmon energy ($\hbar\omega_p$), the force constants (α and β) and the lattice energy (U) for some groups $A^{II}B^{VI}$ and $A^{III}B^{V}$ semiconductors, can be given by the following relations. [24]

$$\hbar\omega_p(\mathrm{eV}) = K_1 \exp(K_2 n), \tag{10}$$

$$\alpha(\mathrm{N/m}) = K_3 \exp(K_4 n), \tag{11}$$

$$\beta(\mathrm{N/m}) = 0.28(1 - f_i)\alpha, \tag{12}$$

$$U(\mathrm{kcal/mol}) = K_5 + K_6 \exp(K_7 n) - K_8 \exp(K_9 n), \tag{13}$$

The relevant values of the different constants K_1, K_2, K_3, K_4, K_5, K_6, K_7, K_8, and K_9 for $A^{III}B^{V}$ groups are respectively: 47.924, – 0.3546, 286.3, – 0.6028, 421.224, 616.88, – 0.1779, 86.771 and – 0.3558.

The f_i is the ionicity of the semiconductor, the rele-vant value of f_i for BP compound will be calculate hereafter (it is equal 0.383). The results for: the plasmon energy, force constants, and lattice energy are presented in Table 3.

The plasmon energy, versus the bond length d, and versus the average energy gap E_g for some groups II-VI, III-V and I-VII materials, can be given by the following relations [27].

$$d(\text{Å}) = C(\hbar\omega_p)^{-2/3}, \tag{14}$$

$$E_g(\mathrm{eV}) = -K_{10} + K_{11}(\hbar\omega_p), \tag{15}$$

The relevant values of the different constants C, K_{10} and K_{11} for $A^{III}B^{V}$ groups are respectively: 15.30, 6.3943 and 0.7678.

From the relations of Eqs. (14) and (15), we can obtain the following expressions:

$$\hbar\omega_p = (C/d)^{3/2}, \tag{16}$$

$$\hbar\omega_p = (E_g + K_{10})/K_{11}, \tag{17}$$

The results for: the plasmon energy, obtained from the relations of equations (16), and (17) by using the bond length d (1.955 Å) [28], and the average energy gap E_g (1.20 eV), obtained from first principles calculation of this work, are respectively: 21.894 eV and 9.891 eV. These two values are generally in agreement with the previous results (15.545 eV, and 16.078 eV) obtained from the application of Eq. (10).

The plasmon energy, can be also given as function of some others parameters: homopolar energy (E_h), heteropolar energy (E_c), ionicity (f_i), and dielectric constant (ε) by the following relations [27].

$$E_h = K_{12}(\hbar\omega_p)K_{13}, \tag{18}$$

$$E_C = K_{14} \exp[K_{15}(\hbar\omega_p)], \tag{19}$$

$$f_i = K_{16} - K_{17}(\hbar\omega_p), \tag{20}$$

$$\varepsilon = K_{18} - K_{19}(\hbar\omega_p), \tag{21}$$

The relevant values of the different constants K_{12}, K_{13}, K_{14}, K_{15}, K_{16}, K_{17}, K_{18}, and K_{19} for $A^{III}B^{V}$ groups are respectively: 0.0509, 1.6192, 0.5093, 0.1199, 0.1809, – 0.0126, 24.9501, and 0.9350.

The results for: homopolar energy (E_h), heteropolar energy (E_c), ionicity (f_i) and dielectric constant (ε), obtained from the relations of equations (18), (19, (20), (21), and the value (16.078 eV) of the plasmon energy are respectively: 1.325 eV, 3.500 eV, 0.383 and 9.917.

These results are given in Table 3, and compared with the available theoretical data [5, 29-32].

Table 3 – Some physical parameters calculated of (B3) BP compound. [a]from the relation (8), [b]from the relation (9), [c]using the refractive index obtained from the relation (8), [d] using the refractive index obtained from the relation (9), [e]from the relation (16), [f] from the relation (17)

Parameter	Our work	Other works
n	3.175[a] 3.080[b]	3.34[5] 1.960[29]
$\hbar\omega_p$ (eV)	15.545[c] 16.078[d] 21.894[e] 9.891[f]	21.71[30]
α (N/m)	42.231[c] 44.720[d]	
β (N/m)	7.296[c] 7.726[d]	
Ionicity	0.383	0.444[29] 0.312[30]
U (kcal/mol)	743.854[c] 748.867[d]	
E_h (eV)	1.325	
E_c (eV)	3.500	
ε	9.917	8.75[31] 11[32]

From the data of the Table 3, it can be seen that our calculated value of the dielectric constant (ε), is in good agreement with the theoretical data [31, 32], and the deviations being 13.33 %, and 9.84 % respectively.

3.3 Sound Velocity, Debye Temperature and Melting Temperature

Sound velocities in BP material are strongly dependent on the propagation directions. If the crystal density g and the stiffness constant C_{ij} of a solid are known, one can calculate the bulk sound velocity v from the following general relation: [23]

$$v = (C_{ij}/g)^{1/2}, \tag{22}$$

In general there are three types of wave motion for a given direction of propagation in the solid crystal, but only for a few special directions can the waves be classified as pure longitudinal or pure transverse. [23]

If we neglect nonlinear terms in the equation of motion, pure longitudinal sound waves may propagate in the [100], [110], and [111] directions [23].

We can see in table 3.25 of Ref. [23] definition of

sound velocity expressed in terms of these constants along the high-symmetry directions [100], [110] and [111] in cubic, zincblende crystals.

The numeric values for g is equal 3.0135 g/cm^3[28], and C_{ij} used in the calculations are taken from Table 1. The predicted values of sound velocities for major directions at zero-pressure are reported in Table 4, and compared with the available theoretical data [11].

Table 4 – Sound velocities for major directions in the (B3) lattice of BP, as controlled by the second-order elastic cons-tants C_{ij}. [a]Longitudinal acoustic waves, [b]Transverse acoustic waves

Propagation (Direction)	Plane of Polarization	Sound Velocity (10^5 cm/s)	
		Our work	Other works
[100]	[100][a]	10.882	10[11]
	(100)[b]	8.0366	7.3[11]
[110]	[100][a]	12.733	11[11]
	[001][b]	8.0366	7.3[11]
	$[1\bar{1}0]$[b]	6.7345	6.0[11]
[111]	[111][a]	12.003	11 [11]
	(111)[b]	7.1947	6.5[11]

The Debye temperature (θ_D) can be obtained by using the following equation [33]

$$\theta_D = \frac{h}{k_B}\left(3/4\pi V a\right)^{1/3} v_m , \qquad (23)$$

where h is the Plank's constant, k_B the Boltzmann's constant and V_a the atomic volume. The average sound velocity is given by [33]

$$v_m = \left[\frac{1}{3}\left(\frac{2}{v_t^3}+\frac{1}{v_l^3}\right)\right]^{-1/3} , \qquad (24)$$

where v_l and v_t are the longitudinal and transverse sound velocity. They are obtained from the Navier's equation [33]

$$v_l = \left(\left(3B+4C_s\right)/3g\right)^{1/2}, \text{ and } v_t = \left(C_s/g\right)^{1/2} \qquad (25)$$

The calculated sound velocity and Debye temperature as well as the density for (B3) BP are given in Table. 5. Unfortunately, to the best of our knowledge, there is a little experimental [34-36], and theoretical [37, 38] data available in the literature on this properties for this compound.

The Debye temperature calculated is in excellent accordance with data available in the literature [34-38], it is deviates from the measured [34] and the calculated [38] ones within ~ 0.01 % and 1.78 % respectively. This marked result signified the good values obtained for the second-order elastic constants C_{ij}.

The melting point of a substance depends usually on pressure and is usually specified at standard atmospheric pressure [39]. The melting temperature of several cubic crystalline solid, can be estimated accor-ding to the following empirical relation between the melting temperature and the elastic constants [40]

$$T_m = 533 + \left(591/\text{Mbar}\right)C_{11} \pm 300\text{K} , \qquad (26)$$

Recently, Kumar et al. [38] proposed a linear relation between the Debye temperature and the melting temperature T_m for some groups II-VI, III-V and I-VII materials, it is given by the following formula:

$$T_m = (\theta_D + K_{20})/K_{21} , \qquad (27)$$

The values of the constants K_{20} and K_{21} are, respectively: 153.40 and 0.354 for A^{III}-B^V semiconductors.

Using eqs. (26) and (27), the values of T_m for (B3) BP compound at equilibrium lattice parameter have been calculated, the results obtained are estimated at 2641.69 ± 300 K, and 3201.69 K respectively. These values are presented in table.5, and compared with the available theoretical data [23, 34, 38, 41]. These values are in general in agreement with the previous calculations data, they are deviate from the value 2863.77 of the others [38] within 7.75% and 11.80% respectively.

Table 5 – Longitudinal, transverse and average sound velocity (v_l, v_t, v_m in 10^3 m/s), the Debye temperature (θ_D in K), and the melting temperature (T_m in K) for (B3) BP in comparison with data available in the literature [11, 23, 34 - 38, 41]. [a]from the relation of equation (26), [b] from the relation of equation (27).

Parameter	Our work	Other works
v_l	10.8821	10[11]
v_t	6.7345	7.3[11]
v_m	7.4266	
θ_D	980.4	980[34] 985[35, 36] 1096[37] from 726.5 to 962.78[38]
T_m	2641.69 ± 300[a] 3201.69[b]	> 3300[23] 2800[34] from 2508.89 to 2863.77[38] 2250[41]

4. CONCLUSION

The results obtained of elastic stiffness constants C_{ij} are very similar to the other experimental and theoretical data of the literature. The values obtained of the elastic constants were used to predict the anisotropy effect for directions within the impo-rtant crystallographic planes on the other parameters such as: sound velocity, young's modulus and poisson's ratio.

The energy band structure at equilibrium lattice parameter and the profile valence density charge along the ⟨111⟩ direction of this compound are also determined. The minimum of the conduction band is found to be at the Δ_{min}, rendering this compound an indirect semiconductor with a $\Gamma_{15v} \rightarrow \Delta_{min}$ optical tran-sition of 1.20 eV. This value is in very good agreement comparatively with the results of the literature.

Other optoelectronic properties of (B3) BP are determined and compared with the other theoretical data. The results obtained for some of these para-meters are generally very similar to the results of other references.

In general, the results obtained of the Debye temperature and the melting temperature agree well with other experimental and theoretical data.

REFERENCES

1. R.M. Wentzcovitch, M. L. Cohen, *Phys. Rev. B* **36**, 6058 (1987).
2. W.R.L. Lambrecht, B. Segall, *Phys. Rev. B* **43**, 7070 (1991).
3. A. Zaoui, F.El Haj Hassan, *J. Phys. Condens. Mat.* **13**, 253 (2001).
4. B. Bouhafs, H. Aourag, M. Ferhat, M. Certier, *J. Phys. Condens. Mat.* **11**, 5781 (1999).
5. W. Wettling, J. Windscheih, *Solid State Commun.* **50**, 33 (1984).
6. H. Meradji, S. Drablia, S. Ghemid, H. Belkhir, B. Bouhafs, A. Tadjer, *phys. status solidi b* **241**, 2881 (2004).
7. P. Rodríguez-Hernández, M. González-Diaz, A. Muñoz, *Phys. Rev. B.* **51**, 14705 (1995).
8. F. Elhajhassan, H. Akbarzadeh, M. Zoaeter, *J. Phys. Condens. Mat.* **16**, 293 (2004).
9. S.Q. Wang, H. Q. Ye, *phys. status solidi b* **240**, 45 (2003).
10. M. Ferhat, A. Zaoui, M. Certier, H. Aourag, *Physica B* **252**, 229 (1998).
11. S. Adachi, *Handbook on Physical Properties of Semiconductors* (Kluwer Academic Publishers: Boston: 2004).
12. W. Kohn, L.J. Sham, *Phys. Rev.* **140**, A1133 (1965).
13. X. Gonze. et al., *Comp. Mater. Sci.* **25**, 478 (2002).
14. X. Gonze, G.M. Rignanese, M. Verstraete, et al., *Z. Kristallogr.* **220**, 558 (2005).
15. S. Goedecker, M. Teter, J. Hutter, *Phys. Rev. B* **54**, 1703 (1996).
16. N. Troullier, J.L. Martins, *Phys. Rev. B* **43**, 1993 (1991).
17. H.J. Monkhorst, J.D. Pack, *Phys. Rev. B* **13**, 5188 (1976).
18. C. Kittel, *Introduction to Solid State Physics, 7ed* (John Wiley & Sons: New York: 1996**)**.
19. O.H. Nielsen, R.M. Martin, *Phys. Rev. B* **32**, 3792 (1985).
20. L. Kleinman, *Phys. Rev.* **128**, 2614 (1962).
21. W.A. Harrison, *Electronic Structure and the Properties of Solids* (Freeman San Francisco: San Francisco: 1980).
22. P. Han, G. Bester, *Phys. Rev. B* **83**, 174304 (2011).
23. S. Adachi, *Properties of Group-IV, III-V and II-VI Semiconductors* (John Wiley & Sons Ltd.: England: 2005).
24. R.R. Reddy, Y.N. Ahammed, P. Abdul Azeem, K.R. Gopal, B.S. Devi, T.V.R. Rao, *Defence. Sci. J.* **53**, 239 (2003).
25. V. Kumar, J.K. Singh, *IJPAP* **48**, 571 (2010).
26. P.J. Herve, L.K.J. Vandamme, *J. Appl. Phys.* **77**, 5476 (1995).
27. V. Kumar, A.K. Shrivastava, Anita Sinha, Vijeta Jha, *IJPAP* **51**, 49 (2013).
28. S. Daoud, K. Loucif, N. Bioud, N. Lebgaa, L. Belagraa, *Pramana J. Phys.* **79**, 95 (2012).
29. D.S. Yadav, C. Kumar, J. Sigh, Parashuram, G. Kumar, *J. Eng. Comput. Innov.* **3** No2, 26 (2012).
30. R.R. Reddy, Y.N. Ahammed, K.R. Gopal, T.V. Rao, B.S. Devi, P. Abdul Azeem, *Indian J. Phys.* **77**A, 237 (2003).
31. A.S. Verma, Naresh Pal, B.K. Sarkar, R. Bhandari, V.K. Jindal, *Phys. Scr.* **85**, 015705 (2012).
32. T. Takenaka, M. Takigawa, K. Shohno, *Jpn. J. App. Phys.* **15**, 2021 (1976).
33. Z. Sun, D. Music, R. Ahuja, S. Li, J.M. Schneider, *Phys. Rev. B.* **70**, 092102 (2004).
34. D.R. Lide (Ed.), *Handbook of Chemistry and Physics* (80thed: CRC Publication: 1999-2000).
35. E.F. Steigmeier, *Appl. Phys. Lett.* **3**, 6 (1963).
36. O. Madelung (Ed.), *Numerical Data and Functional Relationships in science and Technology- Crystal and solid state physics*, *Vol.3* (Landolt-Börnstein, Springer: Berlin: 1972).
37. S. Narain, *phys. status solidi b* **182**, 273 (1994).
38. V. Kumar, V. Jha, A.K. Shrivastava, *Cryst. Res. Technol.* **45**, 920 (2010).
39. J.A. Ramsay, *J. Exp. Biol.* **26**, 57 (1949).
40. S. Cui, W. Feng, H. Hu, Z. Feng, Y. Wang, *Comp. Mater. Sci.* **47**, 968 (2010).
41. J.A. Van Vechten, *Phys. Rev. Lett.* **29**, 769 (1972).